NEUTRON STAR FORMATION IN THEORETICAL SUPERNOVAE — LOW MASS STARS AND WHITE DWARFS —

Ken'ichi Nomoto
Physics Department, Brookhaven National Laboratory; on leave from the Department of Earth Science and Astronomy, University of Tokyo

ABSTRACT: The presupernova evolution of stars that form semi-degenerate or strongly degenerate O+Ne+Mg cores is discussed. For the 10 - 13 $M_\odot$ stars, behavior of off-center neon flashes is crucial. The 8 - 10 $M_\odot$ stars do not ignite neon and eventually collapse due to electron captures. Properties of supernova explosions and neutron stars expected from these *low mass progenitors* are compared with the Crab nebula. We also examine the conditions for which neutron stars form from accretion-induced collapse of white dwarfs in close binary systems.

1. INTRODUCTION

1.1 Neutron Star Formation in 8 - 13 $M_\odot$ Stars

Low mass stars are defined here as stars that form an electron degenerate core during the cource of evolution. The evolution and the final fate of these low mass stars are completely different from more massive stars becasue of the difference in the gravothermal nature of the stars as will be described in §2. Through the study of such *low mass stars*, we can determine the lowest mass of stars that form neutron stars. The stars that form a degenerate C+O core, i.e., 0.5 - 8 $M_\odot$ stars, will become white dwarfs or be completely disrupted by carbon deflagration and, hence, will not form a neutron star. What about slightly more massive, 8 - 13 $M_\odot$, stars? These stars form a strongly degenerate or semi-degenerate O+Ne+Mg core and their evolution will be discussed in §3 - §5. Supernova explosion from the progenitors in this mass range is interesting because it may be the origin of the Crab nebula in view of elemental abundances. The white dwarf is also a potentail neutron star progenitor if it belongs to a close binary system. This possibility will be the subject of §6 - §9 with the following motivation.

1.2 Neutron Star Formation from Accretion-Induced Collapse of White Dwarfs

The final fate of accreting white dwarfs will be either thermonuclear explosion or collapse to form a neutron star, if the white dwarf mass grows to the Chandrasekhar mass. The exploding white dwarf model, in particular, the carbon deflagration

D. J. Helfand and J.-H. Huang (eds.), The Origin and Evolution of Neutron Stars, 281–303.

model is in good agreement with many of the observed features of Type Ia supernovae (Nomoto 1986a; Woosley and Weaver 1986b). For Type Ib supernovae, though currently most popular models are explosions of Wolf-Rayet stars, there is a suggestion that the maximum light spectrum can better be explained by off-center explosions of white dwarfs. Recent observations of several interesting binary systems, low mass X-ray binaries, QPOs, and binary radio pulsars have suggested that in these systems a neutron star has formed from accretion-induced collapse of a white dwarf (van den Heuvel 1984; Taam and van den Heuvel 1986).

These variations in the final fate of accreting white dwarfs originate from the differences in the parameters of the binary system, i.e., composition, mass, and age of the white dwarf, its companion star, and, in particular, mass accretion rate. It is important to know under what condition white dwarfs will collapse to form neutron stars.

Possible models for the white dwarf collapse involve solid C+O white dwarfs, in which carbon and oxygen may or may not have chemically separated (Canal and Isern 1979; Isern et al. 1983) and O+Ne+Mg white dwarfs (Nomoto et al. 1979). For a wide range of mass accretion rates and initial white dwarf masses, the O+Ne+Mg white dwarfs collapse due to electron capture on ^{24}Mg and ^{20}Ne (Nomoto 1980; Miyaji et al. 1980). On the other hand, depending on the conditions of the white dwarfs and binary systems in which they are formed, the C+O white dwarfs could either explode or collapse. Chemical separation in such objects is still hypothetical and in any case could not be complete before carbon burning starts (Mochkovici 1980). It takes a carbon fraction of only a few percent to sustain a deflagration. Therefore, it is worth determining the critical condition for which a carbon deflagration induces the collapse of a C+O white dwarf rather than its explosion.

In §6, the fate of accreting white dwarfs are summarized in the parameter space of accretion rate and the initial mass of the white dwarfs. In §7, models for Type Ia and Ib supernovae are briefly presented. In §8, possibilities of white dwarf collapse is examined. The companion stars, the fate of merging white dwarfs, etc. are discussed in §9.

2. EVOLUTION AS A FUNCTION OF STELLAR MASS

2.1 Effects of Electron Degeneracy on Stellar Evolution

The hydrostatic stellar structure gives a relation between P_c, ρ_c, and stellar mass, M, as $P_c^3/\rho_c^4 \sim M^2$, (Sugimoto and Nomoto 1980; Arnett 1978). For an ideal gas, this gives $T_c^3/\rho_c \sim M^2$. The specific entropy, s, is then given as

$$(\mu H/k)s_c = \ln(T_c^{3/2}/\rho_c) + C_1 = \ln(M^2/T_c^{3/2}) + C_2 = \ln(M/\rho_c^{1/2}) + C_3, \qquad (1)$$

where μ is the mean molecular weight, H atomic mass unit, k Boltsmann constant, and C_1, C_2, and C_3 additional constants. Equation (1) shows that for the same T_c

https://doi.org/10.1017/S0074180900160905 Published online by Cambridge University Press

(i.e, roughly for the same nuclear burning stage), s_c is higher (and ρ_c is lower) for larger M. We need higher entropy to sustain a larger mass against self-gravity.

When nuclear reactions are not active, the star loses entropy by radiation and neutrinos and s_c decreases. Equation (1) shows that both T_c and ρ_c increase as s_c decreases for fixed M. In other words, the specific heat in the central region is negative as $c_g \equiv ds_c/d\ln T_c = -1.5k/\mu H$. The increase in ρ_c implies that the star contracts and releases gravitational energy, a part of which goes into internal energy and the rest goes into radiation and neutrino losses.

The sign of the *specfic heat* depends on the equation of state, however. It is *positive* if electrons are degenerate and the pressure does not depend much on temperature. In this case, the loss of entropy hardly induces gravitational contraction, so that T_c decreases as the star loses energy, i.e., $c_g > 0$. Such a change in equation of state occurs for stars with sufficiently low central entopy and thus for a sufficiently small mass, M, or small core mass, M_{core}, as seen from Eq.(1).

The example of the evolutionary change in the central density and temperature during the gravitational contraction is shown in Figure 1 for neon stars with neon burning artificially suppressed (Nomoto 1984a, 1986a). At the maximum temperature, c_g changes its sign because of electron degeneracy. The maximum temperature is higher for larger M. (For evolved cores, the temperature peak appears not in the center but in the outer shell because of neutrino losses. See §3). We see that there exists a minimum mass for the peak temperature to reach the ignition temperature of the nuclear fuel. The minimum masses are 0.08, 0.25, 1.06, and 1.37 $M_\odot$ for hydrogen, helium, carbon, and neon burning, respectively (e.g., Arnett 1978; Nomoto 1981 for a review). Therefore, stars with a core mass, M_{core}, smaller than the above minimum mass will not undergo further nuclear burning, but form a white dwarf-like degenerate core. In this sense, the stellar mass, M, is a critical parameter to determine the final fate of evolution.

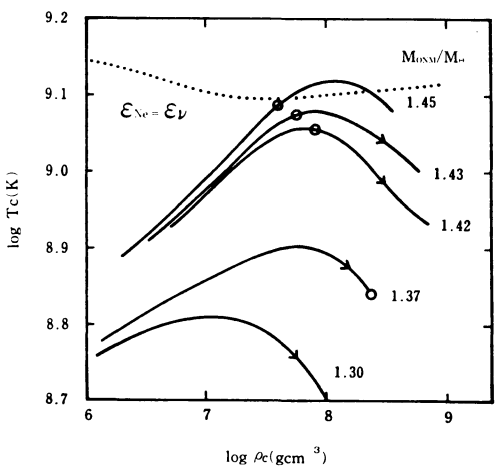

Figure 1: Evolutionary change in the central density and temperature of *neon* stars of mass 1.30 - 1.45 $M_\odot$ during gravitational contraction (Nomoto 1986a). The open circles indicate the stage where the neon ignition temperature (shown by the dotted line) is reached in the outer shell, not in the center. (Further evolution is followed by supressing neon burning.) For stars of mass smaller than 1.37 $M_\odot$, no neon ignition occurs.

https://doi.org/10.1017/S0074180900160905 Published online by Cambridge University Press

2.2 Evolution As a Function of Stellar Mass

In Figure 2, the evolution of the central density, ρ_c, and temperature, T_c, is shown for helium stars (or cores) of mass M_α = 8, 6, 3.3, 3.0, 2.8, and 2.2 $M_\odot$ which correspond to the main-sequence mass of M_{ms} = 25, 19, 13, 12, 11, and 9 $M_\odot$, respectively (Nomoto and Hashimoto 1986). The line for $\psi = 10$ approximately divides the electron degenerate and non-degenerate region, where ψ is the chemical potential of an electron in units of kT. These evolutionary paths clearly indicate the effect of electron degeneracy and its dependence of stellar mass. We can classify the stellar evolution by M as follows:

(1) For $M < 0.08\ M_\odot$, the star will become a planet-like black dwarf without igniting hydrogen burning.
(2) For $0.08\ M_\odot < M < 0.45\ M_\odot$, the star will end up as a helium white dwarf, though such a single star has not evolved off the main-sequence in a Hubble time.
(3) For $0.45\ M_\odot < M < 8\ M_\odot$, the star forms a C+O core of mass smaller than $1.06\ M_\odot$, which then become strongly degenerate. Most of them will become a C+O white dwarf by losing their hydrogen-rich envelope, but some of them (~ 6 - $8\ M_\odot$) could reach a supernova stage by increasing the C+O core mass to the Chandrasekhar mass and ignites a carbon deflagration. The explosion will look like a Type II-L supernova (Doggett and Branch 1985).
(4) For $8\ M_\odot < M < 10\ M_\odot$, an O+Ne+Mg core is smaller than $1.37\ M_\odot$ so that it becomes strongly degenerate. The star will eventually collapse due to electron capture on ^{24}Mg and ^{20}Ne as discussed in §4.
(5) For $10\ M_\odot < M < 13\ M_\odot$, neon is ignited in a semi-degenerate O+Ne+Mg core. Whether subsequent evolution leads to a non-degenerate or a degenerate configuration depends on neutronization during oxygen burning and crucial for their final fate. This question is answered in §3.
(6) For $M > 13\ M_\odot$, the star undergo non-degenerate burning to form an iron core.

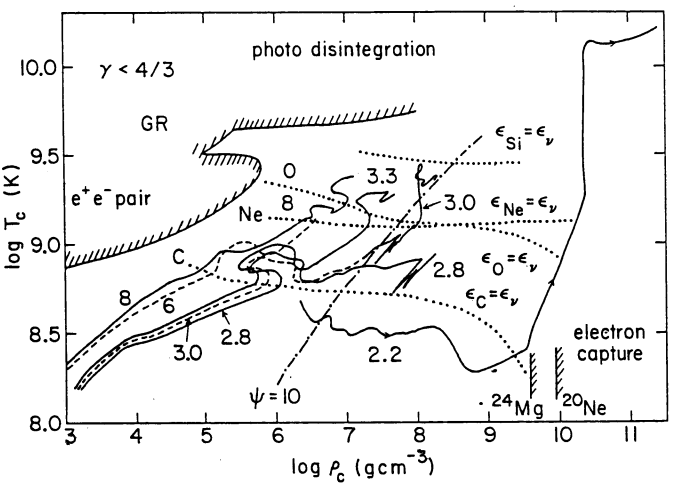

Figure 2: Evolution of the central density, ρ_c, and temperature, T_c for helium stars of mass M_α = 8, 6, 3.3, 3.0, 2.8, and 2.2 $M_\odot$. The approximate ignition lines for carbon, neon, oxygen, and silicon, where the nuclear energy generation rate is equal to neutrino energy losses, are shown.

https://doi.org/10.1017/S0074180900160905 Published online by Cambridge University Press

3. PRESUPERNOVA EVOLUTION OF 10 - 13 $M_\odot$ STARS

3.1 Semi-Degenerate Oxygen-Neon Core and Off-Center Neon Ignition.

The evolution of stars in the mass range of $M_{\rm ms} = 10$ - 13 $M_\odot$ ($M_\alpha \simeq 2.5$ - 3.2 $M_\odot$) is complicated and sensitive to the stellar mass. These stars undergo non-degenerate carbon burning and form an oxygen-neon core whose mass, $M_{\rm ONe}$, is in the range of 1.37 - 1.5 $M_\odot$. The core mass $M_{\rm ONe}$ is large enough to ignite neon, yet the core is semi-degenerate (i.e, $\psi > 10$ in the central region) and the degree of degeneracy depends sensitively on how close $M_{\rm ONe}$ is to the Chandrasekhar mass.

One of the distinct features of a semi-degenerate core is the appearance of a temperature inversion in the central region. This is because neutrino energy losses are faster at higher densities and the degenerate electrons provide the pressure necessary to sustain hydrostatic equilibrium. As a result, neon burning ignites not in the center, but in the outer shell. The location of the neon ignition is $M_{\rm r,ig} = 0.78$ - 0.10 $M_\odot$ for $M_\alpha = 2.6$ - 3.2 $M_\odot$ (Hashimoto and Nomoto 1986; Nomoto 1984a; Habets 1985, 1986). For $M_\alpha = 3.3$ $M_\odot$ ($M_{\rm ms} \sim 13$ $M_\odot$), electron degeneracy is so weak that no temperature inversion appears and neon ignites at the center.

3.2 Propagation of Neon-Oxygen Burning Layer

When neon and oxygen ignite off-center, a sharp temperature jump forms. Subsequently the neon/oxygen burning shell propagates inward (Figure 3). An important question is whether or not the burning shell reaches the center. If not, a degenerate oxygen-neon core is left unburned (Barkat et al. 1974; Woosley and Weaver 1986a)

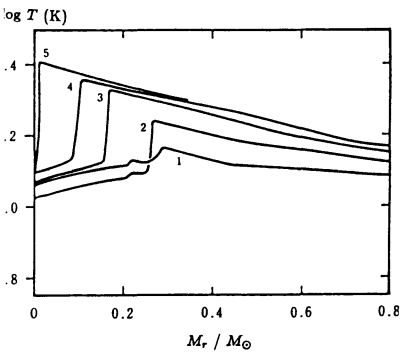

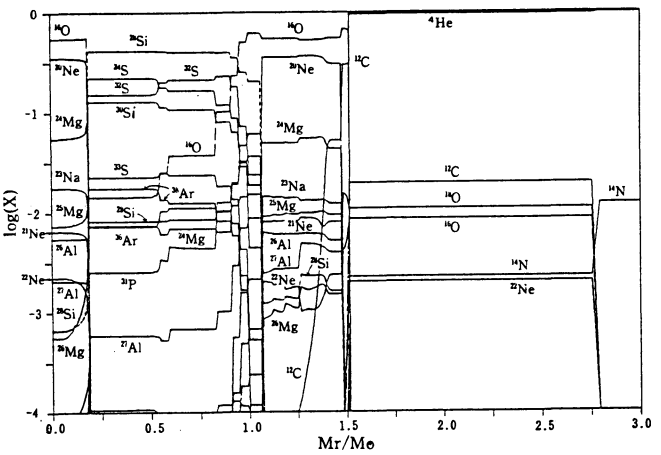

Figure 3 (left): Change in the temperature profile during the propagation of the neon burning front (from stage 1 to 5) for $M_\alpha = 3.0$ $M_\odot$.

Figure 4 (right): Composition of the helium star of $M_\alpha = 3.0$ $M_\odot$ at the shell neon and oxygen burning. The Si-S layer is somewhat neutronized.

https://doi.org/10.1017/S0074180900160905 Published online by Cambridge University Press

and the final fate would be similar to 8 - 10 $M_\odot$ stars. On the other hand, if all neon/oxygen burn, the star will evolve as a non-degenerate massive star and form an iron core.

To answer this question, we have to understand the propagation mode of neon burning front. It is not heat conduction but compressional heating due to gravitational contraction of the oxygen-neon core. If the core mass is larger than a certain critical mass, $c_g < 0$ until T_c reaches the neon ignition temperature. If the core mass is smaller, the temperature decreases ($c_g > 0$) to quench neon burning because of electron degeneracy. For the simple neon star models with the electron mole number $Y_e = 0.5$, this critical mass is 1.44 $M_\odot$ as seen from Figure 1.

For $M_\alpha = 3.0\ M_\odot$ ($M_{ms} \sim 12\ M_\odot$), M_{ONe} is larger than 1.44 $M_\odot$ so that the burning front propagates all the way to the center in 2 yr (Fig. 3). Since the density at the neon burning front does not become so high ($\rho < 10^8$ g cm^{-3}) and also neon ignites layer by layer, the released energy in O-Ne flash is too small to induce major dynamical effects.

For slightly smaller mass of $M_\alpha = 2.8\ M_\odot$ ($M_{ms} \sim 11\ M_\odot$), on the other hand, $M_{ONe} = 1.42\ M_\odot$ so that neon burning will be quenched if Y_e were 0.5. However, the density of the oxygen burning front is as high as 10^8 g cm^{-3} so that Y_e decreases to ~ 0.48 due primarily to electron capture on ^{33}S and ^{35}Cl (Figure 4). This implies that the core mass exceeds the Chandrasekhar mass, which is now ~ 1.38 $M_\odot$, so that c_g remains negative. Therefore, the central temperature will continue to increase up to neon ignition and the burning layer will reach the center. This leads to an important consequnce: the neon burning front reaches densities as high as $\rho > 10^8$ g cm^{-3}. Then the neon shell flashes become so explosive that a dynamical event, such as ejection of a helium layer, is expected (Woosley et al. 1980; Hashimoto and Nomoto 1986).

In short, the propagation of the oxygen-neon shell burning is self-sustanined in the sense that neutronization in the burning layer promotes further contraction. Therefore, the quenching of neon burning and the resulting formation of a strongly degenerate oxygen-neon core would be the case only for very limited mass range, if it occurs at all. Most stars of 10 - 13 $M_\odot$ will evolve to form an iron core and, in particular, 10 - 11 $M_\odot$ stars would undergo very exlosive off-center neon flashes.

4. PRESUPERNOVA EVOLUTION OF 8 - 10 $M_\odot$ STARS

The evolution of 8 - 10 $M_\odot$ stars ($M_\alpha \simeq 2.0$ - $2.5\ M_\odot$) converges to the common path once electrons become strongly degenerate (Nomoto 1984a,b). The representative evolutionary path of (ρ_c, T_c) for a helium core of $M_\alpha = 2.2\ M_\odot$ is seen in Figure 2. Chemical evolution of the core through the beginning ($M_\alpha = 2.4\ M_\odot$) and the end ($M_\alpha = 2.2\ M_\odot$) of the dredge-up of a helium layer is shown in Figures 4 and 5, respectively.

https://doi.org/10.1017/S0074180900160905 Published online by Cambridge University Press

4.1 Formation of Strongly Degenerate O-Ne-Mg Cores

The star in this mass range undergoes non-degenerate carbon burning and forms an O+Ne+Mg core. The advance of the carbon burning shell stops near the helium burning shell at $M_r = 1.28\ M_\odot$ ($M_\alpha = 2.2\ M_\odot$) and $1.34\ M_\odot$ ($M_\alpha = 2.4\ M_\odot$) (Fig. 4 - 5). Hence the oxygen-neon core mass does not exceed the critical mass of $1.37\ M_\odot$ and, therefore, neon is never ignited. After attaining the maximum temperature, which is far below the ignition temperature of neon, T_c decreases due to neutrino emission. Clearly $c_g > 0$, which is an important difference from more massive stars. Afterwards, the core becomes strongly degenerate.

If the core mass stays constant ($\sim 1.3\ M_\odot$), the degenerate core will simply continue to cool like a white dwarf. In a red-giant, the core mass M_{Heb} (defined as the mass interior to the helium burning shell) grows because hydrogen and helium shell burning processes the material of the hydrogen-rich envelope into carbon-oxygen. (The helium layer has been dredged up by the penetrating surface convection zone as seen in Figure 4). In this sense, the core is essentially the same as accreting white dwarfs. As M_{Heb} grows, degenerate electrons get more relativistic, i.e., in the equation of state of $P \sim \rho^{(4+\delta)/3}$, δ changes from 1 to 0. Then ρ_c increases quickly as $\rho_c \sim M_{\mathrm{Heb}}^{2/\delta}$.

4.2 Collapse of O+Ne+Mg Core induced by Electron Captures

When M_{Heb} grows to $1.38\ M_\odot$, ρ_c reaches 4×10^9 g cm^{-3}. Then degenerate electrons provide another effect on stellar evolution, i.e., the electron Fermi energy exceeds the threshold for electron captures ^{24}Mg (e^-, ν) ^{24}Na (e^-, ν) ^{24}Ne and

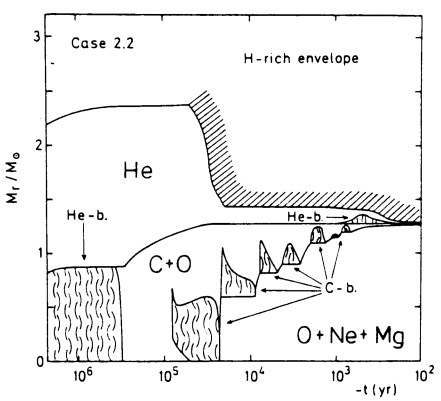

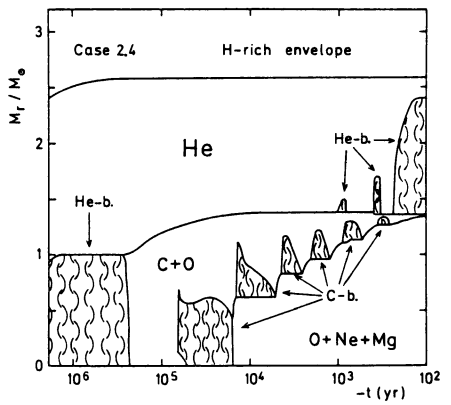

Figure 5 (left): Chemical evolution of the core of $\sim 9\ M_\odot$ star ($M_\alpha = 2.2\ M_\odot$) through the end of the dredge-up of helium layer.

Figure 6 (right): Chemical evolution of the core of $\sim 10\ M_\odot$ star ($M_\alpha = 2.4\ M_\odot$) through the onset of the dredge-up of helium layer.

https://doi.org/10.1017/S0074180900160905 Published online by Cambridge University Press

later for ^{20}Ne (e^-, ν) ^{20}F (e^-, ν) ^{20}O. Electron captures produce entropy by distorting the Fermi distribution function and emitting γ-rays (Bisnovatyi-Kogan and Seidov 1970; Sugimoto 1970). The question is whether this heating ignites oxygen burning. We have found that heating due to ^{24}Na (e^-, ν) ^{24}Ne is slower than the plasmon neutrino cooling but electron capture on ^{20}Ne and ^{20}F leads to the ignition of oxygen at $\rho_c \sim 10^{10}$ g cm^{-3} (Miyaji et al. 1980; Nomoto 1984b; Miyaji and Nomoto 1986). However, the oxygen deflagration does not lead to explosion because the decrease in Y_e due to electron capture behind the burning front is fast enough to induce collapse.

The hydrodynamical behavior of collapse is somewhat different from the iron core collapse of more massive stars (see, e.g., Hillebrandt et al. 1984; Burrows and Lattimer 1985; Baron et al. 1986). The O+Ne+Mg core contains nuclear fuel which ignites during infall. Electron captures occur only in the nuclear statistical equilibrium (NSE) layer behind the burning front and, therefore, the region of small Y_e is confined to a central region which grows gradually. The collapse is slower than the collapse of the iron core of a massive star until the burning front has propagated to roughly $\sim 0.8\ M_\odot$ (Hillebrandt et al. 1984). Afterwards the collapse accerelates quickly. Y_e in the NSE region of the O+Ne+Mg core is smaller than Y_e in iron cores, because the entropy at the burning front is higher and thus the proton fraction is larger. These two effects result in a homologous core whose mass is smaller and an outer infalling layer which is less dense than is the case in iron core collpase. Such a structure has two effects on the bounce shock. First, the binding energy of the rebounding core is smaller and, hence, the shock wave is initially weaker (Brown et al. 1982; Lattimer et al. 1985). Secondly, the low density in the outer layers makes the shock propagation easier (Hillebrandt et al. 1984). Which effect dominates depends on the details of collapse hydrodynamics.

5. SUPERNOVAE and NEUTRON STARS from LOW MASS PROGENITORS

5.1 Neutron Star Mass Inferred from Stellar Structure

Though the hydrodynamic models of collapse and bounce are subject to uncertainties, we can infer some properties of supernovae and neutron stars produced from *low mass* progenitors. Let us compare the density distributions of helium stars of $M_\alpha = 2.4$ and $2.8\ M_\odot$ ($M_{\rm ms} \simeq 10$ and $11\ M_\odot$) with that of $8\ M_\odot$ ($M_{\rm ms} \simeq 25\ M_\odot$). The differences are clearly seen in Figures 7 - 9. Stars forming strongly degenerate or semi-degenerate O+Ne+Mg cores develop a remarkable core-halo structure. The boundary between the *core* and *halo* is located at the helium burning shell. The *core mass* $M_{\rm Heb}$, i.e, mass interior to the helium burning shell, at the precollapse stage is $1.38\ M_\odot$ for $M_\alpha < 2.5\ M_\odot$ and $M_{\rm Heb} = 1.42$, 1.52, and $1.70\ M_\odot$ for $M_\alpha =$ 2.8, 3.0, and $3.2\ M_\odot$, respectively. On the other hand, for non-degenerate massive stars, that feature is much less pronounced.

https://doi.org/10.1017/S0074180900160905 Published online by Cambridge University Press

Suppose that these *low mass stars* give rise to Type II supernova explosions. The mass of a neutron star residue depends on the explosion energy and thus not certain yet. However, we see from the core-halo structure that even a very weak explosion can eject the extended hydrogen-helium layer. Therefore the mass of a neutron star must be less than 1.38 $M_\odot$ (baryon mass) for 8 - 10 $M_\odot$ stars and smaller than 1.4 - 1.7 $M_\odot$ for 10 - 13 $M_\odot$ stars. The baryon mass of 1.4 $M_\odot$ correspond s to the gravitational mass of $\sim$ 1.3 $M_\odot$. Therefore, we can rule out the 8 - 10 $M_\odot$ stars from the progenitors of binary radio pulsars PSR1913+16 because their masses are 1.38 $M_\odot$ and 1.44 $M_\odot$ (e.g., Burrows and Woosley 1986).

5.2 Abundance of the Ejecta

What about the elemental abundances of the ejecta? Composition structures near the neon ignition for $M_\alpha = 2.8\ M_\odot$ and near the end of oxygen burning $M_\alpha = 3.0$ and 8 $M_\odot$ are seen in Figures 10, 4, and 11, respectively. If the supernova explosions form a neutron star of mass $M_{\rm NS}$ (baryon mass), they eject a heavy element mantle of mass ($M_{\rm Heb} - M_{\rm NS}$) and a helium envelope. Though $M_{\rm NS}$ depends on the explosion energy, it is likely to be the mass interior to the oxygen burning shell, which is slightly larger than the iron core mass, becasue rather steep density gradient forms there (e.g., Sugimoto and Nomoto 1980; Woosley and Weaver 1986b).

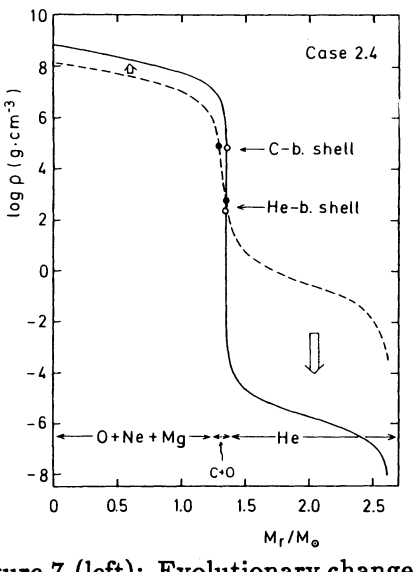

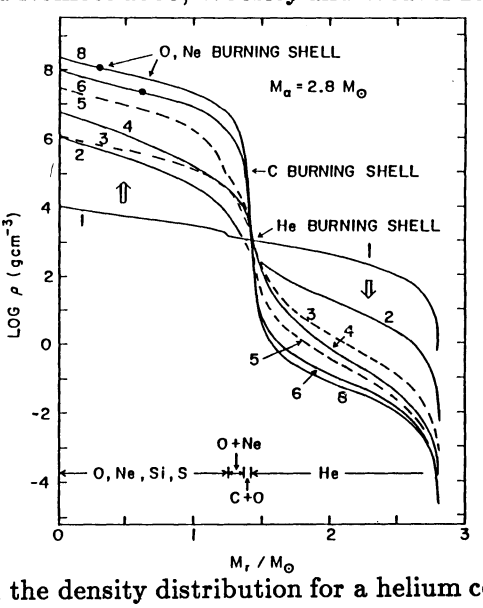

Figure 7 (left): Evolutionary change in the density distribution for a helium core of $M_\alpha = 2.4\ M_\odot$.

Figure 8 (right): Evolutionary change in the density distribution for $M_\alpha = 2.8\ M_\odot$. The stage numbers correspond to 1: exhaustion of helium, 2: ignition of carbon burning, 3: exhaustion of carbon, 4-5: development of a temperature inversion in the O-Ne core, 6: off-center ignition of neon, 7-8: propagation of the neon burning layer.

https://doi.org/10.1017/S0074180900160905 Published online by Cambridge University Press

Then $M_{\rm NS} \simeq 1.35$ - $1.42\ M_\odot$ for $M_\alpha < 4\ M_\odot$ ($M_{\rm ms} < 15\ M_\odot$) (Woosley and Weaver 1986a,b). On the other hand, $M_{\rm Heb}$ and, thus, the ejected mantle mass are sensitive to the stellar mass and smaller for smaller M_α. This is an important feature to compare with the elemental abundances of supernova remnants. In particular, there is no significant overabundance of heavy elements in the Crab nebula relateive to the solar values (Davidson and Fesen 1985 and references therein). This would rule out the stars more massive than 12 $M_\odot$ ($M_\alpha > 3\ M_\odot$) from the Crab nebula's progenitor (Arnett 1975; Woosley et al. 1980; Nomoto et al. 1982; Hillebrandt 1983; Nomoto 1985). If $M_{\rm NS} \simeq 1.35\ M_\odot$ in baryon mass for $M_\alpha < 3\ M_\odot$ (Woosley and Weaver 1986a,b), 8 - 10 $M_\odot$ stars would be favored. Moreover, if we take the carbon abundance obtained from the UV observations as a constraint (Davidson

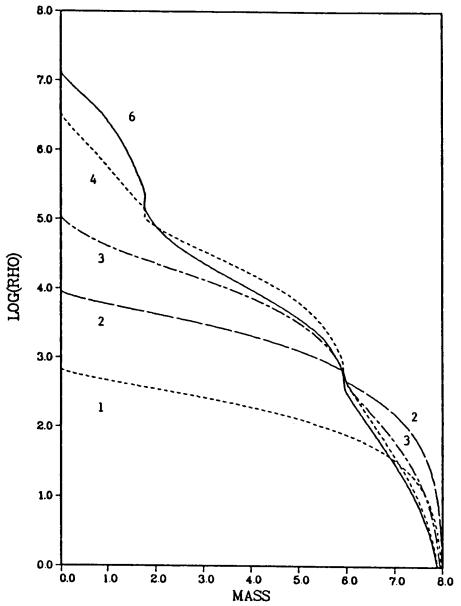

Figure 9

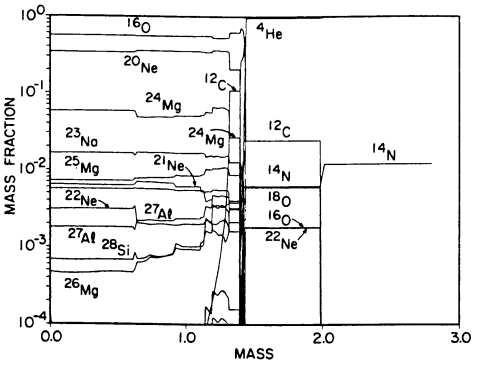

Figure 10

Figure 9: Evolutionary change in the density distribution for the helium star of $M_\alpha = 8\ M_\odot$. Stage numbers refer to: 1) helium burning, 2) helium exhaustion, 3) carbon ignition, 4) neon ignition, 6) oxygen exhaustion.

Figure 10: Compostion of the helium star of $M_\alpha = 2.8\ M_\odot$ near the neon ignition at $M_r = 0.64\ M_\odot$.

Figure 11: Composition of the helium star of $M_\alpha = 8\ M_\odot$ near the end of oxygen burning.

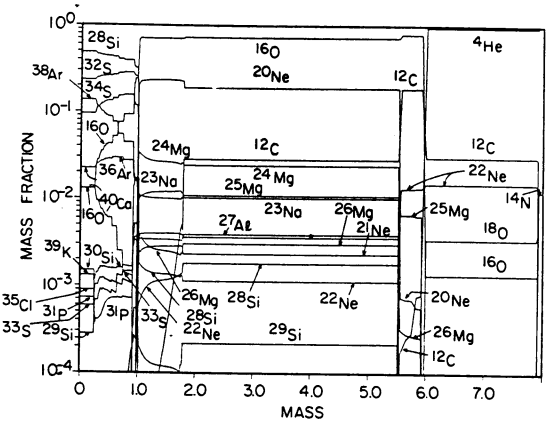

Figure 11

https://doi.org/10.1017/S0074180900160905 Published online by Cambridge University Press

et al. 1982), stars of $M_{ms} \sim 9\ M_\odot$ ($M_\alpha \sim 2.2\ M_\odot$; Fig. 5) would be the likely progenitor because the helium layer of more massive models contain significant amount of carbon as seen in Figures 4, 10, and 11. (Nomoto et al. 1982). On the other hand, if we take little enhancement of nitrogen as a more important constraint, stars of $M_{ms} \sim 10\ M_\odot$ ($M_\alpha \sim 2.4\ M_\odot$; Fig. 6) would be favored (Henry 1986; Nomoto et al. 1982).

5.3 Supernova Light Curve and Pulsar Activity

SN 1054 showed a bright optical display with a tail observed for almost 2 yr. What was the energy source of the light curve? The progenitor was expected to be a red-supergiant and thus had a very extended envelope. Therefore the peak light can be accounted for by the shock heating of photoshpere like Type II supernovae (Chevalier 1977). For the tail, possible energy sources are the decay of ^{56}Ni (which is likely to be the case for some Type II supernovae as well as Type Ia supernovae) and the pulsar activity. From the composition structure, it is clear that the stars smaller than $\sim 15\ M_\odot$ do not produce enough ^{56}Ni. Therefore progenitor models with mass smaller than $15\ M_\odot$ require the pulsar activity as an energy source for the tail (e.g., Chevalier 1977). This implies that the Crab's neutron star should have strong magnetic field and rapid rotation at its birth. If these requirement cannot be fulfilled, we have to invoke the ^{56}Ni decay to explain the light curve tail of SN 1054. This would imply that most of heavy elements formed dust.

6. THE FATE OF WHITE DWARFS AS A FUNCTION OF MASS AND ACCRETION RATE

Isolated white dwarfs are simply cooling stars that eventually end up as *dark matter*. In binary systems they evolve differently because mass accretion from their companion provides gravitational energy that rejuvenates them. The gravitational energy released at the accretion shock near the stellar surface is radiated away and does not heat the white dwarf interior. However, the compression of the interior by the accreted matter releases additional gravitational energy. Some of this energy goes into thermal energy (compressional heating) and the rest is transported to the surface and radiated away (radiative cooling). Therefore, the interior temperature is determined by the balance between heating and cooling and, thus, strongly depends on the mass accretion rate, $\dot{M}$ (Nomoto 1982, 1984b).

Compression first heats up a layer near the surface because of the small pressure scale height there. Later, heat diffuses inward. The diffusion timescale depends on $\dot{M}$ and is small for larger $\dot{M}$'s because of the large heat flux and steep temperature gradient generated by rapid accretion. For example, the time it takes the heat wave to reache the central region is about 2×10^5 yr for $\dot{M} \sim 10^{-6}\ M_\odot\ \mathrm{yr}^{-1}$ and 5×10^6 yr for $\dot{M} \sim 4 \times 10^{-8}\ M_\odot\ \mathrm{yr}^{-1}$. Therefore, if the initial mass of the white dwarf, M_{CO}, is smaller than $1.2\ M_\odot$, the entropy in the center increases substantially due

https://doi.org/10.1017/S0074180900160905 Published online by Cambridge University Press

to the heat inflow and carbon ignites at relatively low central density ($\rho_c \simeq 3 \times 10^9$ g cm^{-3}). On the other hand, if the white dwarf is sufficiently massive and cold at the onset of accretion, the central region is compressed only adiabatically and thus is cold when carbon burning is ignited in the center. In the latter case, the ignition density is as high as 10^{10} g cm^{-3} (e.g., Isern et al. 1983).

Accordingly, the ultimate fate of accreting C+O white dwarfs depends on $\dot{M}$ and the inintial mass of the white dwarf M_{CO}, as summarized in Figure 12. $\dot{M}$ denotes the growth rate of the C+O white dwarf mass irrespective of the composition of the accreting matter. A similar diagram for the O+Ne+Mg white dwarfs is shown in Figure 13. *Neutron Star* or *NS* in Figure 12 indicates a region of parameter space where neutron star formation by white dwarf collapse is expected. The evolution of the white dwarfs in these three regions is summarized as follows. (The fate of white dwarfs in other regions in Figure 12 is briefly described in §7.)

1) For $\dot{M} > 2.7 \times 10^{-6}\ M_\odot$ yr^{-1}, off-center carbon burning is ignited by rapid compressional heating as indicated in Figure 14 (Nomoto and Iben 1985; Kawai et al. 1986). The C+O white dwarf is peacefully changed into an O+Ne+Mg white dwarf through off-center carbon burning (Saio and Nomoto 1985; Woosley et al. 1986a). The resulting O+Ne+Mg white dwarf will collapse to form a neutron star due to electron capture on ^{24}Mg and ^{20}Ne if the Chandrasekhar mass is reached.

2) For $2.7 \times 10^{-6}\ M_\odot$ yr$^{-1} > \dot{M} > 4 \times 10^{-8}\ M_\odot$ yr^{-1} and $M_{CO} > 1.2\ M_\odot$, a central density as high as 10^{10} g cm^{-3} is reached by adiabatic compression if the

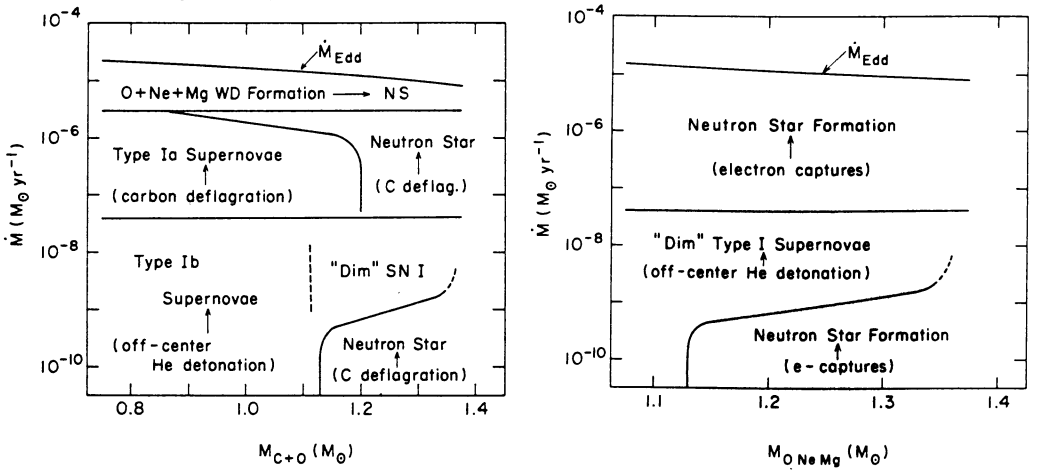

Figure 12 (left): The final fate of accreting C+O white dwarfs expected for their initial mass M_{CO} and accretion rate $\dot{M}$. For two regions indicated by *Neutron Star*, carbon deflagration propagating from $\rho_c \simeq 10^{10}$ g cm^{-3} will induce collapse.

Figure 13 (right): Same as Figure 12 but for O+Ne+Mg white dwarfs. For a wider range of $\dot{M}$ and the initial mass, M_{ONeMg}, neutron star formation triggered by electron capture on ^{24}Mg and ^{20}Ne is expected.

https://doi.org/10.1017/S0074180900160905 Published online by Cambridge University Press

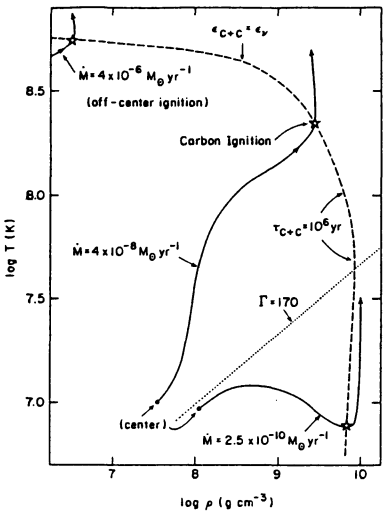

Figure 14: Evolutionary path of (ρ_c, T_c) at the center of accreting C+O white dwarfs for two cases of $\dot{M}$. For comparison, ignition point of off-center carbon burning is shown for $\dot{M} = 4 \times 10^{-6}\ M_\odot\ yr^{-1}$. The dashed curve is an approximate ignition line where the rate of carbon burning ϵ_{C+C} is equal to the rate of neutrino losses ϵ_ν for $T > 2 \times 10^8$ K and $\tau_{C+C} \equiv c_p\ T/\epsilon_{C+C} = 10^6$ yr for $T \leq 2 \times 10^8$ K (c_p is the specific heat).

white dwarf is sufficiently cold at the onset of accretion. For $\dot{M} > 10^{-6}\ M_\odot\ yr^{-1}$, the lower mass limit is not 1.2 $M_\odot$, but 1.0 $M_\odot$.

3) For $\dot{M} \leq 10^{-9}\ M_\odot\ yr^{-1}$ and $M_{CO} > 1.13\ M_\odot$, the white dwarf is too cold to initiate a helium detonation. Eventually pycnonuclear carbon burning starts in the center when ρ_c reaches $\sim 10^{10}$ g cm^{-3}. An evolutionary path of ρ_c - T_c for a model with $\dot{M} = 2.5 \times 10^{-10}\ M_\odot\ yr^{-1}$ and $M_{CO} = 1.16\ M_\odot$ is shown in Figure 14. In this model, the outer layer of 0.24 $M_\odot$ is composed of helium.

7. MODELS FOR SUPERNOVAE OF TYPE Ia AND Ib

7.1 Type Ia Supernovae

For relatively high accretion rates ($2.7 \times 10^{-6}\ M_\odot\ yr^{-1} > \dot{M} > 4 \times 10^{-8}\ M_\odot\ yr^{-1}$), a carbon deflagration starts in the white dwarf's center at a relatively low central density ($\rho_c \sim 3 \times 10^9$ g cm^{-3}) (e.g., Ivanova et al. 1974; Nomoto et al. 1984 and references therein). The *convective* deflagration wave then propagates outward at a subsonic velocity. The density the wave encounters is decreasing due to the expansion of the white dwarf.

The products of explosive nucleosynthesis depend on the temperature and density at the deflagration front and, thus, vary from layer to layer. In the center, iron peak elements are produced. In particular, about 0.6 $M_\odot$ of ^{56}Ni is synthesized. In the outer layers, intermediate mass elements such as Ca, Ar, S, Si are produced. The white dwarf is disrupted completely and no neutron star residue remains (Nomoto et al. 1984; Thielemann et al. 1986; Woosley et al. 1984).

The carbon deflagration model can account for the light curves, early time specta, and late time spectra of Type Ia supernovae as follows (see Nomoto 1986a; Woosley and Weaver 1986b for reviews and references therein):

https://doi.org/10.1017/S0074180900160905 Published online by Cambridge University Press

(1) The theoretical light curve based on the radioactive decays of ^{56}Ni and ^{56}Co into ^{56}Fe fits the observations well.
(2) The synthetic spectum at maximum light is in excellent agreement with the observed spectum of SN 1981b as seen in Figure 15 (Branch et al. 1985; Wheeler and Harkness 1986).
(3) At late times, the outer layers are transparent and the inner Ni-Co-Fe core is exposed. Synthetic spectra of emission lines of [Fe II] and [Co I] agree quite well with the spectra observed at such phase (Woosley et al. 1984).

7.2 Type Ib Supernovae

Recent observations has established the existence of another kind of Type I supernovae, designated Type Ib (SN Ib) (e.g., Wheeler and Harkness 1986 and references therein). The SN Ib spectra are characterized by the lack of the 6125 Å Si feature at maximum light and the appearance of oxygen emission lines at late times (e.g., Gaskel et al. 1986). The currently popular progenitor models for SN Ib are Wolf-Rayet stars (e.g., Wheeler and Levreault 1985; Begelman and Sarazin 1986). However, a large mass of Wolf-Rayet stars may yield a light curve whose decline is too slow to be compatible with SN Ib observations (Wheeler and Levrerault 1985).

Branch and Nomoto (1986) have suggested that the observed spectra are better explained by an accreting white dwarf model. In Figure 16, the maximum-light

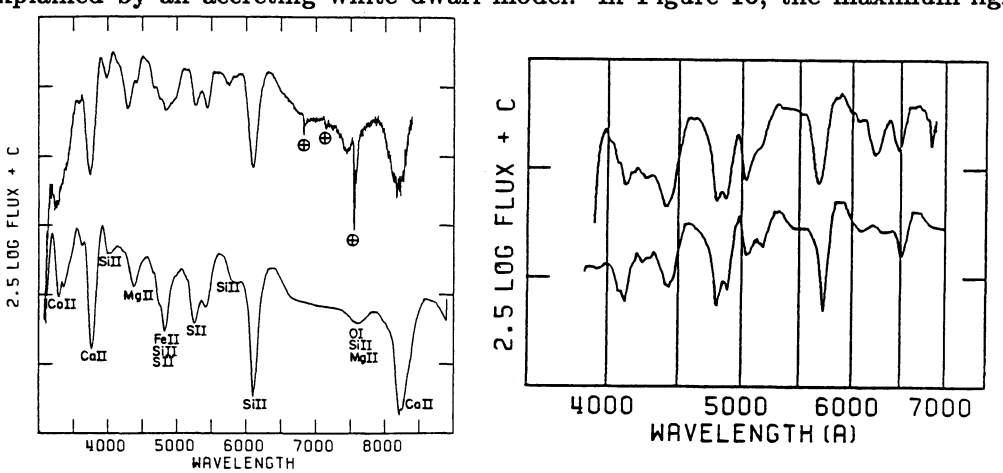

Figure 15 (left): The maximum-light spectrum of SN 1981b (top) is compared to a synthetic spectrum for the carbon deflagration model (Nomoto et al. 1984; Branch et al. 1985). In this model outer layer is assumed to be mixed.

Figure 16 (right): The maximum-light spectrum of the Type Ib SN 1984*l* (upper; Wheeler and Levreault 1985) is compared with a synthetic spectrum (lower; Branch and Nomoto 1986). In the synthetic spectrum the blueshifted absorption component of He I λ6678 appears near 6500 Å and He I λ5876 appears near 5850 Å. Other features are produced primarily by Fe II lines.

https://doi.org/10.1017/S0074180900160905 Published online by Cambridge University Press

spectrum of SN 1984*l* is compared with a synthetic spectrum. Two of the absorption lines in the red are identified as He I lines and other features are well explained as Fe II lines. Here the expansion velocity at the photosphere is 8,000 km s^{-1}. In addition, ultraviolet features can fit with a synthetic spectrum of Co II and Fe I lines if the photoshperic velocity is 12,000 km s^{-1} (Branch and Venkatakrishna 1986). The above interpretation suggests that Fe, Co (decaying), and He are in the outer high-velocity layers and oxygen is in the inner layers.

The existence of such high velocity Fe and, especially, Co is difficult to explain with the Wolf-Rayet model. Branch and Nomoto (1986) have speculated that the progenitors of SN Ib are white dwarfs having $\dot{M} < 4 \times 10^{-8}\ M_\odot\ \mathrm{yr}^{-1}$. Such a slow accretion induces an off-center helium detonation that will occur at a point rather than all over a spherical shell. The outer helium layer will burn to mostly ^{56}Ni with a trace He and the inner C+O core will remain unburned. A part or most of the C+O will be ejected following ^{56}Ni layer. Since the ejected mass of ^{56}Ni will be as small as 0.1 - 0.3 $M_\odot$, the peak luminosity of this model is lower than that for SN Ia by a factor of 2 - 6. This is consisttent with the observations of SN Ib. If the white dwarf accretes matter with an efficiency of only 0.03 - 0.1 from a wind (10^{-6} - $10^{-7}\ M_\odot\ \mathrm{yr}^{-1}$) of a relatively massive (4 - 7 $M_\odot$) red giant companion (Iben and Tutukov 1984), the model would be consistent with relatively young nature of SN Ib. Further, this scenario is consistent with the radio observations of SN Ib in that they can be explained by the interaction of supernova ejecta with the circumstellar shell (Sramek et al. 1984; Chevalier 1984).

7.3 Dim Type I Supernovae

If an off-center *single* detonation occurs on a very massive white dwarf ($> \sim 1.1\ M_\odot$), the resulting supernova will be rather *dim*, because the accumulation of only a small amount of helium ($\sim$ 0.01 - 0.1 $M_\odot$) can lead to the helium detonation. In most cases, an unburned C+O core will be left behind as a white dwarf. Such dim supernovae (Branch and Doggett 1985) are more likely to be associated with O+Ne+Mg white dwarfs since their masses are larger than $\sim 1.2\ M_\odot$.

8. COLLAPSE INDUCED BY CARBON DEFLAGRATION AT HIGH DENSITY

8.1 Conductive Deflagration

As mentioned in §6, there are two scenarios in which a carbon deflagration is initiated in the center when the central density is as high as 10^{10} g cm^{-3}. At such densities, the carbon deflagration may not lead to an explosion since electron capture is much faster at these high densities than at the lower densities encountered in the models of SN Ia. Moreover, if the central part of the white dwarf is in the solid state, the propagation mode of the burning front could be different. If the solid is strong enough, convection will be suppressed and the burning front will

propagate as a *conductive* deflagration wave (Canal et al. 1980; Isern et al. 1983, 1985) though more study is needed on this point. Even for fluid layers, conductive deflagration could dominate convective deflagration in the central region (Woosley and Weaver 1986c). The propagation velocity of a conductive deflagration wave is given approximately by the expression, $v_{\rm def} \sim \delta/\tau_{\rm n} \sim (\sigma/c_{\rm v}\tau_{\rm n})^{1/2}$, where δ denotes the width of burning front, $\tau_{\rm n}$ the nuclear burning timescale, σ the conductivity, and $c_{\rm v}$ the specific heat (Buchler et al. 1980; Woosley and Weaver 1986c). This gives $v_{\rm def} \sim 100$ km s^{-1} at $\rho \sim 10^{10}$ g cm^{-3}, which is about 0.01 $v_{\rm s}$ (Woosley and Weaver 1986c). Here $v_{\rm s}$ is the sound speed, equal to 1.0 - 1.3 $\times$ 10^4 km s^{-1} between $\rho = 10^9$ - 10^{10} g cm^{-3}.

Whether the white dwarf explodes or collapses depends on whether, behind the deflagration wave, nuclear energy release or electron capture is faster. A white dwarf whose mass is close to the Chandrasekhar mass has an adiabatic index close to 3, so that even a small energy release can cause substantial expansion. However, a slight pressure decrease due to electron capture will easily induce collapse. If $v_{\rm def}$ is low (high) enough and/or the central density is high (low) enough, a carbon deflagration will lead to collapse (explosion). The outcome is rather sensitive to $v_{\rm def}$ and the central density.

We have performed numerical simulations of a conductive deflagration started at high central density ($\rho_{\rm c} \simeq 10^{10}$ g cm^{-3}), with $\dot{M} = 2.5 \times 10^{-10}\ M_\odot$ yr^{-1} and

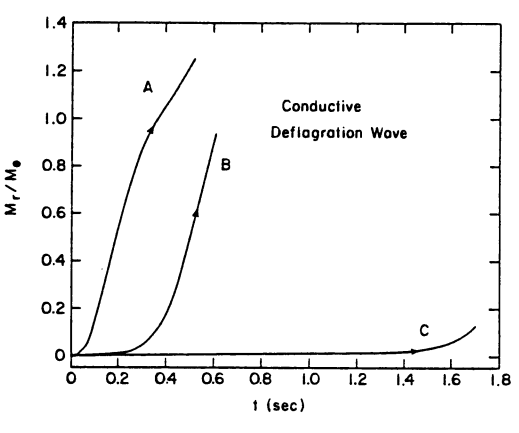

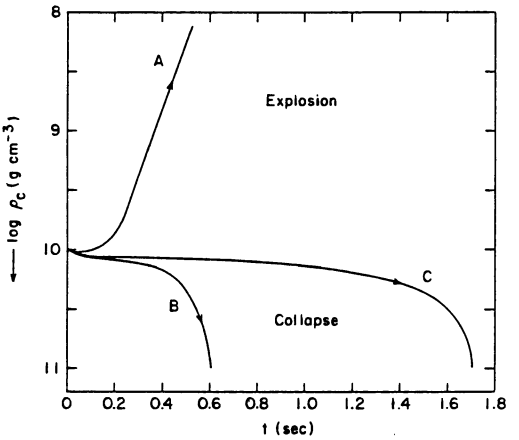

Figure 17 (left): Propagation of the conductive deflagration wave. The location (M_r) of the deflagration front is shown as a function of time, t, for three cases (A, B, C) of parametrized conductivity.

Figure 18 (right): Change in the central density of the white dwarf associated with the propagation of the conductive deflagration wave. Relatively slow propagation in Cases B and C leads to the increase in $\rho_{\rm c}$, i.e., collapse of the white dwarf. On the other hand, faster proapagation in Case A induces the explosion of the white dwarf.

https://doi.org/10.1017/S0074180900160905 Published online by Cambridge University Press

$M_{CO} = 1.16\ M_\odot$ as described in §6 and shown in Figure 14 (Nomoto 1986b). Here we have assumed that no chemical separation occurs. Pycnonuclear carbon burning commences in the solid region and turns into thermonuclear runaway. Then, we have parametrized the conductivity to obtain a range of reasonable v_{def}. With these, we have explored the range of possible hydrodynamical responses of the white dwarf. In Figure 17, the location of the deflagration front as a function of time, t, after initiation is plotted for three cases (A, B, C). In addition, Case D of the slowest propagation has been calculated. The average v_{def}/v_s for Cases A, B, C, and D is about 0.15, 0.1, 0.06, and 0,01, respectively. In Figure 18, the evolution of the central density, ρ_c, for Cases A - C is plotted.

8.2 Cases of Collapse

As Figure 18 indicates, in Case B, the central density *increases* as the deflagration front propagates outward. When the deflagration front has reached $M_r \simeq 0.9\ M_\odot$ ($t \simeq 0.6$ s), ρ_c is as high as 10^{11} g cm^{-3}. Clearly, the white dwarf now undergoes quasi-dynamic contraction because electron capture on NSE elements rapidly reduce the electron mole number, Y_e, behind the deflagration wave. This effect dominates the opposing effect of nuclear burning. (At $t = 0.16$ s, Y_e has dropped to 0.42 at the center.) Moreover, once the contraction of the white dwarf begins, photodissociation becomes important, further promoting collapse. In Case C, the contraction is much more gradual than in Case B because the deflagration wave is slower. When ρ_c reaches 10^{11} g cm^{-3}, the burned mass is only 0.13 $M_\odot$ (Figures 17 and 18). In Case D, for which v_{def} ($\sim 0.01\ v_s$) is close to the actual conductive deflagration speed, it takes 155 s to reach $\rho_c \simeq 10^{11}$ g cm^{-3}. At $t = 155$ s, the mass of the burned region is only 0.03 $M_\odot$ and $Y_e \sim 0.39$.

8.3 Case of Explosion

On the other hand, in Case A, ρ_c decreases as the deflagration propagates outward. By the time the front has reached $M_r \simeq 1.2\ M_\odot$, the total energy of the white dwarf is already 1.2×10^{51} ergs and it is clear that it will be completely disrupted. Nuclear energy release dominates electron capture because the front's density, and hence its electron capture rate, decreases as the front propagates outward. When the deflagration wave arrives at the base of the helium layer ($M_r = 1.16\ M_\odot$), it turns into a helium *detonation* because of a low ignition temperature. The explosion starting from high ρ_c should not be frequent since they eject too much neutron-rich iron peak matter into the Galaxy (Nomoto et al. 1984; Woosley and Weaver 1986c).

8.4 Convective Deflagration

In some cases of carbon ignition at high densities (e.g., $\dot{M} > 4 \times 10^{-8}\ M_\odot$ yr^{-1}), convective deflagration would develop. Even for the solid core, propagation of

the deflagration wave is not necessarily due to conduction alone since convection could influence the melting of the solid core (Mochkovitch 1980). To investigate the outcome of convective deflagration, a set of numerical experiments has been performed for $\rho_c \sim 10^{10}$ g cm^{-3} by employing time-dependent mixing length theory with a parameter $\alpha = \ell / H_p$ where ℓ is the mixing length and H_p is the pressure scale height (Nomoto et al. 1984).

For $\alpha = 0.7$, the propagation velocity is as slow as $v_{def} < 0.11\ v_s$ at $M_r < 0.6\ M_\odot$ so that the white dwarf collapses as in Case B. On the other hand, for $\alpha = 1.0$, $v_{def} > 0.15\ v_s$ at $M_r > 0.4\ M_\odot$ and the white dwarf explodes completely. Since a value for α of 0.7 is preferred in the low density carbon deflagration model of SN Ia (§7), a plausible choice for α in the present context may be 0.7, not 1.0. (For both low and high central densities, the carbon deflagration with $\alpha = 1.0$ grows into a *detonation* in the outer layer and incinerates almost the entire star to the iron peak. This is incompatible with observations of SN Ia (Nomoto et al. 1984).) Therefore, for plausible choices of the α parameter, a carbon deflagration initiated at high densities will result in white dwarf collapse, not explosion.

9. DISCUSSION ON WHITE DWARF COLLAPSE

9.1 C+O White Dwarfs

We have shown how the fate of accreting white dwarfs depends on the initial mass, composition, and age of the white dwarf and accretion rate. In particular, we have examined the critical condition for which a carbon deflagration leads to collapse. If a carbon deflagration is initiated in the center of the white dwarf when $\rho_c \simeq 10^{10}$ g cm^{-3} and if the propagation velocity of the deflagration wave is slower than a certain critical speed, v_{crit}, the outcome is collapse, not explosion (Nomoto 1986b; also Ivanova et al. 1974, Isern et al. 1985). For $v_{def} > v_{crit}$, complete disruption results (and the ejecta contain too much neutron-rich matter). The value of v_{crit} depends on ρ_c at carbon ignition. For $\rho_c \simeq 1 \times 10^{10}$ g cm^{-3}, $v_{crit} \sim 0.15\ v_s$. A lower ρ_c implies a lower v_{crit}. In our case of $\rho_c \simeq 1 \times 10^{10}$ g cm^{-3}, for both conductive and convective deflagrations $v_{def} < v_{crit}$ and, therefore, collpase will result.

Such a high central density is reached in two regions of the $\dot{M}$ - M_{CO} plane of Figure 12. One is defined by $\dot{M} > 4 \times 10^{-8}\ M_\odot$ yr^{-1} and $M_{CO} > 1.2\ M_\odot$, while the other is defined by $\dot{M} < 10^{-9}\ M_\odot$ yr^{-1} and $M_{CO} > 1.13\ M_\odot$. The frequency of such systems may be small. First, if hydrogen-rich matter accretes at $\dot{M} < 10^{-9}$ $M_\odot$ yr^{-1}, nova-like explosions will prevent the white dwarf mass from growing. Secondly, massive C+O white dwarfs ($> 1.2\ M_\odot$) may be rare. The formation of such white dwarfs might be prevented if the precursor star lost its hydrogen-rich envelope by either a stellar wind or Roche-lobe overflow before its degenerate C+O core could grow substantially.

9.2 O+Ne+Mg White Dwarfs

As seen in Figure 13, the accretion-induced collapse is the outcome for a wider range of parameter space for O+Ne+Mg white dwarfs. The initial mass of the white dwarf, $M_{\rm ONeMg}$, is larger than $\sim 1.2\ M_\odot$ (Nomoto 1980, 1984a). In many cases, $M_{\rm ONeMg}$ is very close to the Chandrasekhar mass, so that only a small mass increase is enough to trigger collapse. However, an O+Ne+Mg white dwarf formes from an 8 - 10 $M_\odot$ star (Nomoto 1984a). The number of such systems may be significantly smaller than the number of systems containing C+O white dwarfs whose precursors are 1 - 8 $M_\odot$ stars, perhaps, by four order of magnitude (Iben and Tutukov 1984). Even so, the number of low mass X-ray binaries is much smaller than the number of SN I and the statistics may be consistent (Webbink et al. 1983).

9.3 Companion Star of the White Dwarfs

Among the possible regions of the parameter space for neutron star formation (Figs. 12 - 13), rather high accretion rates ($\dot{M} > \dot{M}_{\rm det}$) are favored in order to avoid nova explosions and helium detonations (e.g., Nomoto 1982). Possibel binary systems to realize such accretion rate include: (1) Case A mass transfer on thermal timescale from a main-sequence star of $\sim 2\ M_\odot$ ($\dot{M} \sim 10^{-7}\ M_\odot\ {\rm yr}^{-1}$) (Iben and Tutukov 1984), (2) mass transfer on the nuclear timescale from a subgiant of $\sim 0.8\ M_\odot$ ($\dot{M} \sim 10^{-7}$ - $10^{-8}\ M_\odot\ {\rm yr}^{-1}$) (Webbink et al. 1983), and (3) accretion of helium from a helium main-sequence star on a timescale of gravitational wave radiation (~ 2 - $3 \times 10^{-8}\ M_\odot\ {\rm yr}^{-1}$) (Savonije et al. 1986; Iben et al. 1986). For Cases 2 - 3, the $^{14}{\rm N}({\rm e}^-, \nu)^{14}{\rm C}(\alpha, \gamma)^{18}{\rm O}$ reaction would be important to lower $\dot{M}_{\rm det}$ from 4×10^{-8} to $1 \times 10^{-8}\ M_\odot\ {\rm yr}^{-1}$ (Hashimoto et al. 1986).

9.4 Single Millisecond Pulsar from Merging Double White Dwarfs?

As mentioned in §6, if the merging of CO - CO white dwarf pair (Iben and Tutukov 1984; Webbink 1984) leads to a rapid accretion such as $\dot{M} > 2.7 \times 10^{-6}\ M_\odot\ {\rm yr}^{-1}$, the final outcome would be a neutron star. This is also the case with the merging of CO - ONeMg white dwarf pair for all range of accretion rates (Kawai et al. 1986). Since the collapsing white dwarf has gained angular momentum during merging, the resulting neutron star is a rapid rotator. Suppose that the magnetic field of a neutron star originates from a fossil field of the white dwarf and no enhancement of the field occurs after the neutron star formation. Then the neutron star could be weakly magnetized if the magnetic field of the white dwarf was weak. (White dwarfs in cataclysmic variables are classified into two classes, with and without strong magnetic field (King et al. 1984).) The neutron star could continue to rotate rapidly for relatively long time. Forthermore, the precursors of CO or ONeMg white dwarfs are 5 - 10 $M_\odot$ stars so that a location of the resulting neutron star may not be far from the galactic plane. These features could be consistent with the properties of the single millisecond pulsar (Baker et al. 1982). On the other hand, if the

magnetic field is enhanced during or after collapse, a normal single pulsar would result but with no supernova remnant around it (see Saio and Nomoto 1985).

9.5 Dim or Silent Supernovae?

A hydrodynamical calculation of a white dwarf collapse has not been carried out so that we don't know whether mass is ejected. Even if no mass is ejected, a neutron star will form because the residue's mass (1.4 $M_\odot$ (baryon mass), $\sim$ 1.3 $M_\odot$ (gravitational mass)) is smaller than the maximum mass of a neutron star. Nevertheless, it is important to know whether some mass is ejected by the bounce shock and, if mass is ejected, what its composition is. If some ^{56}Ni is ejected, the white dwarf collapse can be observed as a *dim* Type I supernova. Otherwise, the collapse would be *silent*, because most of the explosion energy would go into the kinetic energy of expansion. The interior temperatures would be too low to produce a significant optical light curve. If the shock wave is strong enough, some neutron-rich species will be ejected. This might be an important site of some neutron-rich isotopes (Hartman et al. 1985; Takahashi et al. 1986). Mass ejection will affect the binary evolution after the explosion and the results can be compared to the observed neutron star binary systems (e.g., Taam and van den Heuvel 1986).

I would like to thank Drs. Hashimoto, D. Branch, J.C. Wheeler, R. Harkness, and Z. Barkat for informative discussion on massive star evolution and Type I supernovae. It is a pleasure to thank Drs. S.H. Kahana, G.E. Brown, A. Yahil, A. Burrows, J. Cooperstein, and E. Baron for useful discussion and hospitality during my stay in Brookhaven and Stony Brook. This work has been supported in part by the U. S. Department of Energy under Contract No. DE-AC02-76CH00016 and the Japanese Ministry of Education, Science, and Culture through research grant Nos. 59380001 and 60540152.

REFERENCES

Arnett, W.D. 1975, *Ap. J.*, *195*, 727.
————. 1978, in *Physics and Astrophysics of Neutron Stars and Black Holes*, ed. R. Giaconni and R. Ruffini (Bologna: Soc. Italiana di Fisica), p.356.
Backer, D.C., Kulkarni, S.R., Heiles, C., Davis, M.M., and Goss, W.M. 1982, *Nature*, *300*, 615.
Barkat, Z., Reiss, Y., and Rakavy, G. 1974, *Ap. J. (Letters)*, *193*, L21.
Baron, E., Cooperstein, J., and Kahana, S.H. 1986, private communication.
Begelman, M.C., and Sarazin, C.L. 1986, *Ap. J. (Letters)*, *302*, L59.
Bisnovatyi-Kogan, G.S., and Seidov, A.F. 1970, *Astr. Zh.*, *47*, 139.
Branch, D., and Doggett, J.B. 1985, *A. J.*, *270*, 2218.
Branch, D., Doggett, J.B., Nomoto, K, and Thielemann, F.-K. 1985, *Ap. J.*, *294*, 619.

Branch, D., and Nomoto, K. 1986, *Astr. Ap.*, in press.
Branch, D., and Venkatakrishna, K.L. 1986 *Ap. J. (Letters)*, *306*, L21.
Brown, G.E., Bethe, H.A., and Baym, G. 1982, *Nucl. Phys.*, *A375*, 481.
Buchler, J.R., Colgate, S.A., and Mazurek, T.J. 1980, *J. de Phys. Suppl. 3*, *41*, C2-159.
Burrows, A., and Lattimer, J.M. 1985, *Ap. J. (Letters)*, *299*, L19.
Burrows, A., and Woosley, S.E. 1986, *Ap. J.*, *308*, in press.
Canal, R., Isern, J., and Labay, J. 1980, *Ap. J. (Letters)*, *241*, L33.
Chevalier, R.A. 1977, in *Supernovae*, ed. D.N. Schramm (Dordrecht: Reidel), p.53.
————. 1984, *Ap. J. (Letters)*, *285*, L63.
Davidson, K., and Fesen, R.A. 1985, *Ann. Rev. Astr. Ap.*, *23*, 119.
Davidson, K., et al. 1982, *Ap. J.*, *253*, 696.
Doggett, L.B., and Branch, D. 1985, *A. J.*, *90*, 2303.
Gaskell, C.M., Cappellaro, E., Dinerste in, H., Garnett, D., Harkness, R.P., and Wheeler, J.C. 1986, *Ap. J. (Letters)*, *306*, L77.
Habets, G.M.H.J. 1985, Ph.D. Thesis, University of Amsterdam.
————. 1986, *Astr. Ap.*, submitted.
Hartmann, D., Woosley, S.E., and El Eid, M.F. 1985, *Ap. J.*, *297*, 837.
Hashimoto, M., and Nomoto, K. 1986, in preparation.
Hashimoto, M., Nomoto, K., Arai, K., and Kaminisi, K. 1986, *Ap. J.*, *307*, in press.
Henry, R.B.C. 1986, *Pub. Astr. Soc. Pacific*, in press.
Hillebrandt, W. 1983, *Astr. Ap.*, *110*, L3.
Hillebrandt, W., Nomoto, K., and Wolff, R.G. 1984, *Astr. Ap.*, *133*, 175.
Iben, I. Jr., Nomoto, K., Tornambe, A., and Tutukov, A.V. 1986, *Ap. J.*, submitted.
Iben, I. Jr., and Tutukov, A.V. 1984, *Ap. J. Suppl.*, *54*, 335.
Isern, J., Labay, J., Hernanz, M., and Canal, R. 1983, *Ap. J..*, *273*, 320.
Isern, J., Labay, J., and Canal, R. 1984, *Nature*, *309*, 431.
Ivanova, L.N., Imshennik, V.S., and Chechetkin, V.M. 1974, *Ap. Space Sci.*, *31*, 497.
Kawai, Y., Saio, H., and Nomoto, K. 1986, *Ap. J.*, submitted.
King, A.R., Frank, J., and Ritter, H. 1985, *M.N.R.A.S.*, *213*, 181.
Lattimer, J.M., Burrows, A., and Yahil, A 1985, *Ap. J.*, *288*, 644.
Miyaji, S., Nomoto, K., Yokoi, K., and Sugimoto, D. 1980, *Pub. Astr. Soc. Japan*, *32*, 303
Miyaji, S., and Nomoto, K. 1986, *Ap. J.*, submitted.
Mochkovitch, R. 1980, Thesis, University of Paris.
————. 1983, *Astr. Ap.*, *122*, 212.
Nomoto, K. 1980, in *Type I Supernovae*, ed. J. C. Wheeler (Austin: University of Texas), p. 164.
————. 1981, in *IAU Symposium 93, Fundamental Problems in the Theory of Stellar Evolution*, ed. D. Sugimoto, D.Q. Lamb, and D.N. Schramm (Dordrecht: Reidel), p.295.
————. 1982, *Ap. J.*, *253*, 798.

Nomoto, K. 1984a, *Ap. J.*, *277*, 791.
————. 1984b, in *Stellar Nucleosynthesis*, ed. C. Chiosi and A. Renzini (Dordrecht: Reidel), p. 205 and p. 238.
————. 1985, in *The Crab Nebula and Related Supernova Remnants*, ed. M.C. Kafatos and R.B.C. Henry (Cambridge Univ. Press), p. 97.
————. 1986a, *Ann. N Y Acad. Sci.*, *470*, 294.
————. 1986b, in *Proceedings of VIth Moriond Astrophysics Meeting: Accretion Processes in Astrophysics*, in press.
Nomoto, K., and Hashimoto, M. 1986, *Prog. Part. Nucl. Phys.*, *18*, in press.
Nomoto, K., and Iben, I Jr. 1985, *Ap. J.*, *297*, 531.
Nomoto, K., Miyaji, S., Yokoi, K., and Sugimoto, D. 1979, in *IAU Colloquium 53, White Dwarfs and Variable Degenerate Stars*, ed. H.M. Van Horn and V. Weidmann (Rochester: Univ. of Rochester), p.56.
Nomoto, K., Sparks, W.M., Fesen, R.A., Gull, T.R., Miyaji, S., and Sugimoto, D. 1982, *Nature*, *299*, 803.
Nomoto, K., Thielemann, F.K., and Yokoi, K. 1984, *Ap. J.*, *286*, 644.
Saio, H., and Nomoto, K. 1985, *Astr. Ap.*, *150*, L21.
Savonije, G.J., de Kool, M., and van den Heuvel, E.P.J. 1986, *Astr. Ap.*, *155*, 51.
Sramek, R.A., Panagia, N., and Weiler, K.W. 1984, *Ap. J. (Letters)*, *285*, L59.
Sugimoto, D. 1970, *Ap. J.*, *161*, 1069.
Sugimoto, D., and Nomoto, K. 1980, *Space Sci. Rev.*, *25*, 155.
Taam, R.E., and van den Heuvel, E.P.J. 1986, *Ap. J.*, *305*, 235.
Takahashi, Y., Miyaji, S., Parnell, T.A., Weisskopf, M.C., Hayashi, T. and Nomoto, K. 1986, *Nature*, *326*, 839.
Thielemann, F.-K., Nomoto, K., and Yokoi, K. 1986, *Astr. Ap.*, *158*, 17.
Van den Heuvel, E.P.J. 1984, *J. Ap. Astr.*, *5*, 209.
Webbink, R. 1984, *Ap. J.*, *277*, 355.
Webbink, R.F. Rappaport, S., and Savonije, G.J. 1983, *Ap. J.*, *270*, 678.
Wheeler, J.C., and Harkness, R. 1986, in *Distances to Galaxies and Deviation from the Hubble Flow*, ed. B.M. Madore and R.B. Tully (Dordrecht: Reidel).
Wheeler, J.C., and Levreault, R. 1985, *Ap. J. (Letters)*, *294*, L17.
Woosley, S.E., Axelrod, R.S., and Weaver, T.A. 1984, in *Stellar Nucleosynthesis*, ed. C. Chiosi and A. Renzini, (Dordrecht: Reidel), p.263.
Woosley. S .E., and Weaver, T.A. 1986a, in *Nucleosynthesis and Its Implications for Nuclear and Particle Physics*, ed. J. Audouze and T. van Thuan (Dordrecht: Reidel).
————. 1986b, *Ann. Rev. Astr. Ap.*, in press.
————. 1986c, in *IAU Colloquium 89, Radiation Transport and Hydrodynamics*, ed. D. Mihalas and K.H. Winkler.
Woosley, S.E., Weaver, T.A., and Taam, R.E. 1980, in *Type I Supernovae*, ed. J. C. Wheeler (Austin: University of Texas), p. 96.

DISCUSSION

Srinivasan: If the pulsar beaming factor is 5, then the analysis of Blaauw suggests that stars with masses as low as 6 $M_{\odot}$ should produce neutron stars. Could you please comment on this.

Nomoto: The smallest mass of stars that produce neutron stars is often called $M_{\rm UP}$, above which a degenerate O+Ne+Mg core forms. $M_{\rm UP}$ depends on the extent of convective overshooting, or convective core size, during H and He burning. $M_{\rm UP}$ $\sim$ 8 $M_{\odot}$ is obtained from models with negligible overshooting. If the overshooting is significant, $M_{\rm UP}$ could be as low as 5 - 6 $M_{\odot}$ as reported by Italian and Dutch group. However, $M_{\rm UP}$ is quite uncertain because we don't have a good theory of convective overshooting yet.

Bisnovatyi-Kogan: How can you explain theoretically the uniqueness (peculiarity) of the Crab supernova?

Nomoto: The Crab supernova may not be so unique. Increasing number of Crab-like remnants have been observed. The mass range of stars that form O+Ne+Mg cores is rather narrow yet they would produce non-negligible fraction of Type II supernovae because of mass function.

Srinivasan: There are reasons to beleive that the supernova of 1054 was a very low energy explosion. Does this fit to your theoretical picture?

Nomoto: In my scenario, the Crab nebula's progenitor had lost a significant fraction of its hydrogen-rich envelope by wind and became as small as $\sim$ 4 $M_{\odot}$ when it exploded (Nomoto et al. 1982). In other words, the explosion is supposed to be weak and no high velocity hydrogen-rich material is expected. The progenitor was still a red-supergiant with some circumstellar matter so that even a weak explosion could produce observed optical light.

https://doi.org/10.1017/S0074180900160905 Published online by Cambridge University Press